Electrochimica Acta 270 (2018) 165–173

Contents lists available at ScienceDirect

Electrochimica Acta

journal homepage: www.elsevier.com/locate/electacta

Capacitive deionization with wire-shaped electrodes

T.M. Mubita [a, b], S. Porada [b, c], P.M. Biesheuvel [b], A. van der Wal [a, d], J.E. Dykstra [a, b, *]

[a] Department of Environmental Technology, Wageningen University, Bornse Weilanden 9, 6708 WG Wageningen, The Netherlands
[b] Wetsus, European Centre of Excellence for Sustainable Water Technology, Oostergoweg 9, 8911 MA Leeuwarden, The Netherlands
[c] Soft Matter, Fluidics and Interfaces Group, Faculty of Science and Technology, University of Twente, Meander ME 314, 7500 AE Enschede, The Netherlands
[d] Evides, Schaardijk 150, 3063 NH Rotterdam, The Netherlands

ARTICLE INFO

Article history:
Received 19 January 2018
Received in revised form
7 March 2018
Accepted 12 March 2018
Available online 14 March 2018

Keywords:
Capacitive deionization
Dynamic ion adsorption theory
Amphoteric donnan model
Wire-shaped electrodes

ABSTRACT

Capacitive deionization is a desalination technology to remove ions from aqueous solution in a cyclic manner by applying a voltage between pairs of porous electrodes. We describe the dynamics of this process by including a possible rate limitation in the transport of ions from the interparticle pore space in the electrode into intraparticle pores, where electrical double layers are formed. The theory includes the effect of chemical surface charge located in the intraparticle pores, which is present in the form of acidic and basic groups. We present dynamic data of salt adsorption for electrodes with and without coated ion-exchange membranes. Experiments were conducted in a CDI cell geometry based on wire-shaped electrodes placed together. The electrodes consisted of graphite rods coated with a layer of porous carbon. To fabricate this layer, we examined two procedures that involve the use of different solvents: acetone and N-methyl-2-pyrrolidone (NMP). We found that electrodes prepared with acetone had a lower salt adsorption compared to electrodes prepared with NMP. At equilibrium, the theory is in agreement with data, and this agreement underpins the effect of chemical surface groups on electrode performance. Under dynamic conditions, our theory describes reasonably well desalination cycles.

1. Introduction

Water desalination using capacitive deionization (CDI) is based on the removal of ions from aqueous solutions by electrosorption [1–3]. For CDI with porous carbon electrodes, after applying a voltage between the electrodes, cations are adsorbed into the negatively polarized electrode while anions are adsorbed into the positively polarized electrode (adsorption step). When the adsorption capacity of the electrodes is reached, the electrodes can be short-circuited for regeneration and ions are released (desorption step) [4–6]. During desalination two processes jointly occur in the carbon electrodes: ion transport and adsorption. Ions are transported through the interparticle space, the macropores. Ion adsorption occurs in the intraparticle space, the micropores, where electrical double layers (EDLs) are formed [7–9].

Several mathematical models describe adsorption phenomena in EDLs. The Helmholtz and Gouy-Chapman-Stern models are well-known [10–12], but do not accurately describe ion adsorption for CDI [13]. The Donnan model and its extended versions, however, describe ion adsorption to a very accurate degree [13–15]. The latest version of the Donnan model, the amphoteric Donnan (amph-D) model, includes the effect of charged surface groups in EDLs [16,17]. These charged surface groups are present in the form of acidic groups, e.g., carboxyl structures, or basic groups, e.g., amine structures. Different from previous Donnan models [13,15,18,19], the amph-D model does describes the sometimes-observed phenomenon of ion desorption at the start of an adsorption cycle [20–22].

In the present work, we use the amph-D model and couple it to a transport theory to dynamically describe the desalination process. In the transport theory, we include a transport limitation for ions between macro- and micropores. This approach is different from the often-used assumption of infinitely fast ion adsorption into micropores [8,23–25].

To compare our dynamic theory with experimental data, we use a CDI cell with rod-shaped electrodes ("wire-CDI cell"), Fig. 1a. The wire-CDI cell is a simple cell design (compared to conventional CDI), which consists of graphite rods (wires) coated with a thin porous carbon layer [26]. To enhance salt adsorption, we coat ion-exchange membranes (IEMs) on the carbon layer. The inclusion of

* Corresponding author. at: Department of Environmental Technology, Wageningen University, Bornse Weilanden 9, 6708 WG Wageningen, The Netherlands. .
E-mail address: jouke.dykstra@wur.nl (J.E. Dykstra).

https://doi.org/10.1016/j.electacta.2018.03.082

Nomenclature

A_e	Outer electrode area, cathode or anode (m^2)
c_{ions}	Average ion concentration in micropores (mM)
c_{mA}	Salt concentration in macropores (mM)
$c_{mA,i}$	Ion concentration in macropores (mM)
c_{mi}	Ion concentration in micropores (mM)
C_S	Stern later capacitance (F/m^3)
F	Faraday's constant (C/mol)
j	Transfer rate of ions between macro- and micropores ($mol/m^3/s$)
J_{charge}	Ionic current density ($mol/m^2/s$)
J_{ions}	Flux of ions ($mol/m^2/s$)
k	Rate constant (1/s)
M_e	Total mass of porous carbon layer, cathode and anode (g)
M_w	Molecular weight (g/mol)
p_{mA}	Macroporosity
p_{mi}	Microporosity
V_{bulk}	Volume bulk solution (m^3)
V_{cell}	Cell voltage (V)
V_e	Electrode volume (m^3)
V_{mA}	Volume of macropores (m^3)
V_T	Thermal voltage (V)
α	Volume fraction of A- and B-region
κ_D	Conductance of the bulk solution (m/s)
κ_{mem}	Membrane transport rate constant (m/s)
λ	Thickness carbon layer (m)
ρ_{elec}	Electrode mass density (g/m^3)
Σ_F	Charge (C/g)
υ_{mi}	Micropore volume (m^3/g)
$\Delta\phi_{bulk}$	Potential drop over the bulk solution (−)
$\Delta\phi_D$	Donnan potential (−)
$\Delta\phi_{EDL}$	Electrical double layer potential (−)
$\Delta\phi_{mem}$	Potential drop over the membrane (−)
$\Delta\phi_S$	Stern potential (−)
σ_{chem}	Chemical surface charge (mM)
σ_{elec}	Electric charge (mM)
σ_{ionic}	Ionic charge (mM)
ωX	Membrane charge density (mM)

IEMs in the system is referred to as membrane capacitive deionization (MCDI) [9,27]. The carbon layer on the electrodes is prepared by mixing activated carbon with a polymeric binder dissolved in an organic solvent. Often, N-methyl-2-pyrrolidone (NMP) is used as a solvent [8,26]. In this work, we tested a new method to fabricate the carbon layer by using acetone as solvent. Acetone is a less toxic alternative to NMP [28,29]. In addition, acetone evaporates faster than NMP, which decreases the preparation time of the electrodes.

One of our aims is to present a modified theory to dynamically describe salt adsorption and charge storage in CDI and MCDI. Our theory is not only valid for wire-CDI systems, but can also be applied to other CDI cell designs and to other electrosorption processes. In this paper, we validate the theory with experiments conducted with wire-shaped electrodes with and without coated IEMs. Furthermore, we compare salt adsorption and charge storage of porous carbon electrodes prepared with two different organic solvents, acetone and NMP.

2. Theory

In this Section we present: i) the theory used to calculate salt adsorption and charge in equilibrium, when there is no transport of ions either through the macropores or from macro- to micropores, and ii) our dynamic theory to describe electrosorption.

2.1. Equilibrium theory

To describe salt adsorption in equilibrium for CDI, we use the amphoteric Donnan (amph-D) model [16,30]. This model includes the effect of charged surface groups in EDLs. These groups are fixed to the carbon surface and can be formed during the activation process of the carbon material or during cell operation [31–33]. In each electrode, we model two different micropore regions: the A- and B-region. The A-region contains acidic groups, such as carboxyl-, lactone- or phenol- groups [34]. The B-region contains basic groups (i.e., protonated groups). In the A- and B-region, three types of charge are present: i) electronic charge in the carbon matrix, σ_{elec}, ii) ionic charge in the micropores, σ_{ionic}, and iii) chemical surface charge fixed to the carbon surface, σ_{chem}. Each region is overall charge neutral, thus

$$\sigma_{elec,j} + \sigma_{ionic,j} + \sigma_{chem,j} = 0 \tag{1}$$

where subscript j refers to region A or B. Charge $\sigma_{chem,\,A}$ has a negative sign, and $\sigma_{chem,\,B}$ has a positive sign.

Similar to the classical Donnan model [18,35], the amph-D model also considers overlapping EDLs and assumes that the electric potential inside the micropores, in each region, does not depend on distance to the pore wall. Therefore, the concentration of ion i in a micropore region j, $c_{mi,i,j}$ can be related to the concentration in the macropores, $c_{mA,i}$, according to the Boltzmann equilibrium

$$c_{mi,i,j} = c_{mA,i} \cdot \exp(-z_i \cdot \Delta\phi_{D,j}) \tag{2}$$

where parameter z_i is the charge number of an ion, and $\Delta\phi_{D,j}$ the dimensionless Donnan potential.

From now on, we consider an electrolyte containing only a dissolved 1:1 salt in water, such as NaCl. In the macropores, we assume electroneutrality, which is given by

$$c_{mA,cation} = c_{mA,anion} = c_{mA} \tag{3}$$

while the ionic charge in each micropore region is

$$\sigma_{ionic,j} = c_{mi,cation,j} - c_{mi,anion,j}. \tag{4}$$

The Stern layer, which is located between the carbon surface and the aqueous phase in the micropore, is considered in the amph-D model. The Stern layer potential, $\Delta\phi_{S,j}$, is related to the Stern layer capacitance, C_S, and $\sigma_{elec,j}$ according to

$$\sigma_{elec,j} \cdot F = V_T \cdot \Delta\phi_{S,j} \cdot C_S \tag{5}$$

where F is Faraday's constant, and V_T the thermal voltage ($V_T = RT/F$).

The potential drop over the EDL, $\Delta\phi_{EDL}$, is the sum of the Stern and Donnan potentials and (in a given electrode) is equal for the acidic and basic region

$$\Delta\phi_{EDL} = \Delta\phi_{D,A} + \Delta\phi_{S,A} = \Delta\phi_{D,B} + \Delta\phi_{S,B}. \tag{6}$$

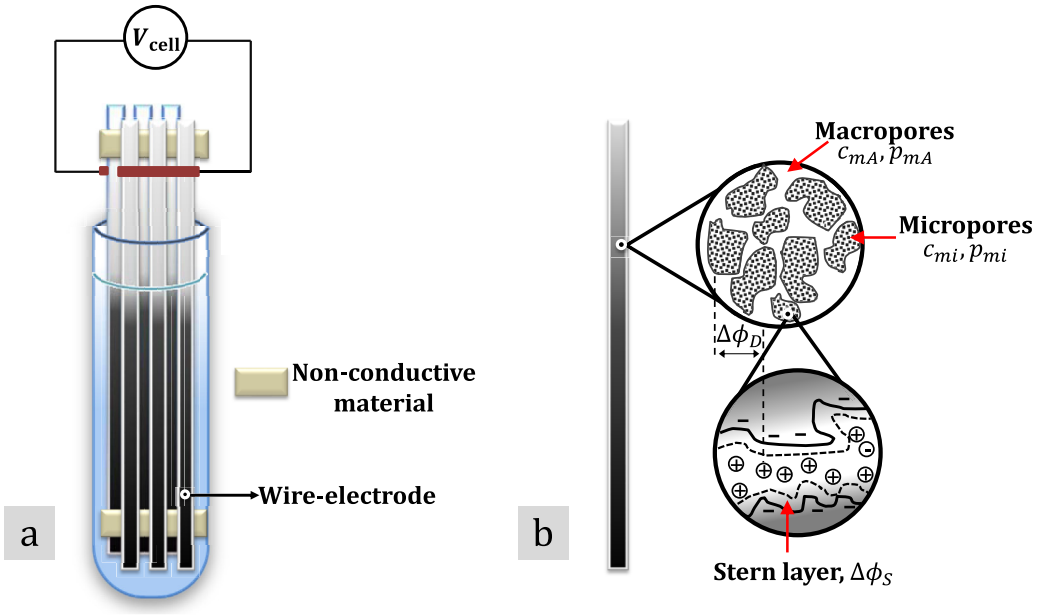

Fig. 1. a) Capacitive deionization cell used in this study. The cell consists of three pairs of porous carbon electrodes. Ions are adsorbed from solution upon applying a voltage between pairs of electrodes. b) In the electrodes, ions are adsorbed in electrical double layers formed in the micropores.

For each electrode, the average electronic charge, σ_{elec}, ionic charge, σ_{ionic}, and average ion concentration in the micropores, c_{ions}, are given by

$$\sigma_{elec} = \sum_{j=A,B} \alpha_j \cdot \sigma_{elec,j} \tag{7}$$

$$\sigma_{ionic} = \sum_{j=A,B} \alpha_j \cdot \sigma_{ionic,j} \tag{8}$$

$$c_{mi,ions} = \sum_{j=A,B} \alpha_j \cdot \left(c_{mi,cation,j} + c_{mi,anion,j}\right) \tag{9}$$

where α_j is the fraction of each region relative to the total micropore volume (v_{mi}, mL/g electrode). Note that $\alpha_A + \alpha_B = 1$.

We calculate the charge, Σ_F, from the difference between the micropore charge at the end of the adsorption step (superscript "ads, end") and that at the end of the desorption step (superscript "des, end") [8].

$$\Sigma_F = \tfrac{1}{2} \cdot F \cdot v_{mi} \cdot \left| \sigma_{elec}^{ads,end} - \sigma_{elec}^{des,end} \right|. \tag{10}$$

The salt adsorption is calculated according to

$$\Gamma_{salt} = \tfrac{1}{4} \cdot M_{w,NaCl} \cdot v_{mi} \cdot \left(\left(c_{mi,ions}^{ads,end} - c_{mi,ions}^{des,end} \right)_{ca} + \left(c_{mi,ions}^{ads,end} - c_{mi,ions}^{des,end} \right)_{an} \right) \tag{11}$$

where $M_{w,NaCl}$ is the molecular weight of NaCl. We relate the cell voltage, V_{cell}, to $\Delta\phi_{EDL}$ according to

$$\frac{V_{cell}}{V_T} = \Delta\phi_{EDL,an} - \Delta\phi_{EDL,ca} \tag{12}$$

where subscripts *an* refers to anode and *ca* to cathode.

Equations (1)–(12) describe, together with a mass balance of the cell (see S.I. A), salt adsorption in equilibrium for CDI. For MCDI, however, we need to consider the IEMs. Previous work [26] assumed that the membranes are perfectly selective, which means that co-ions (ions with the same sign as the membrane fixed charge) cannot go through. In our work, we relax this assumption and consider non-ideal permselectivity, which we will describe in Section 2.2.

2.2. Dynamic theory

To model dynamics of ion adsorption from macropores into each micropore region in the electrodes, we use an expression similar to the one used to calculate the transfer rate of electrons in redox reactions at electrode surfaces [36]. However, instead of using this equation for a redox-reaction, in this work, we use it to describe the transfer rate of each type of ion between macro- and micropores, given by

$$j_{i,j} = k \cdot \left(c_{mA} \cdot \exp\left(-\tfrac{1}{2} \cdot z_i \cdot \Delta\phi_{D,j} \right) - c_{mi,i,j} \cdot \exp\left(\tfrac{1}{2} \cdot z_i \cdot \Delta\phi_{D,j} \right) \right) \tag{13}$$

where $j_{i,j}$ is the transfer rate of each type of ion per unit macropore volume into micropore region j (mol/m^3/s), and k is the rate constant which we assume to have the same value for cations and anions.

For monovalent salt solutions, we derive expressions for the transfer rate of ions, j_{ions}, and charge, j_{charge}, between macro- and micropores, expressed in mol/m^3/s

$$j_{ions,j} = j_{cation,j} + j_{anion,j} \tag{14}$$

$$j_{charge,j} = j_{cation,j} - j_{anion,j}. \tag{15}$$

we insert Eq. (13) in Eqs. (14) and (15) to arrive at

$$j_{ions,j} \Big/ k = 2 \cdot c_{mA} \cdot \cosh\left(\tfrac{1}{2} \cdot \Delta\phi_{D,j}\right) - \left[c_{mi,ions,j} \cdot \cosh\left(\tfrac{1}{2} \cdot \Delta\phi_{D,j}\right) + \sigma_{ionic,j} \cdot \sinh\left(\tfrac{1}{2} \cdot \Delta\phi_{D,j}\right) \right] \tag{16}$$

$$j_{charge,j}/k = -2\cdot c_{mA}\cdot\sinh(½\cdot\Delta\phi_{D,j}) - [c_{mi,ions,j}\cdot\sinh(½\cdot\Delta\phi_{D,j}) + \sigma_{ionic,j}\cdot\cosh(½\cdot\Delta\phi_{D,j})]. \quad (17)$$

For both anode and cathode, we set up an ion balance over the macropore volume, which includes the flux of the ion from the bulk solution into the electrode, J_i (mol/m^2/s), and the flux of ions from macro- to micropore, j_i, according to

$$V_{mA}\frac{\partial c_{mA,i}}{\partial t} = A_e\cdot J_i - V_{mA}\sum_{j=A,B} j_{i,j}. \quad (18)$$

where V_{mA} is the total volume of macropores in the anode or cathode, and A_e is the outer area of the electrode. As electroneutrality holds in the macropores, summing Eq. (18) over cat- and anions results in

$$2\cdot\frac{\partial c_{mA}}{\partial t} = \frac{J_{ions}}{p_{mA}\cdot\lambda_e} - j_{ions} \quad (19)$$

where λ_e is the ratio of electrode volume over electrode surface area, $\lambda_e = V_e/A_e$, p_{mA} is the macroporosity, and where J_{ions} *and* j_{ions} are given by

$$J_{ions} = J_{cation} + J_{anion} \quad (20)$$

$$j_{ions} = \sum_{j=A,B} j_{ions,j}. \quad (21)$$

In (each region of) the micropores we relate $c_{mi,i,j}$ to $j_{i,j}$ by

$$\alpha\cdot p_{mi}\cdot\frac{\partial c_{mi,i,j}}{\partial t} = p_{mA}\cdot j_{i,j} \quad (22)$$

where p_{mi} is the microporosity.

We substitute Eq. (22) into Eq. (4) to derive a mass balance for $\sigma_{ionic,j}$

$$\alpha\cdot p_{mi}\cdot\frac{\partial\sigma_{ionic,j}}{\partial t} = p_{mA}\cdot j_{charge,j}. \quad (23)$$

The average ionic charge in the micropores, σ_{ionic}, can be related to ionic current density, J_{charge} (mol/m^2 s), which is defined per projected area of an electrode, according to

$$p_{mi}\cdot\frac{\partial\sigma_{ionic}}{\partial t} = \frac{J_{charge}}{\lambda_e}. \quad (24)$$

we relate J_{charge} to the potential drop over the bulk solution, $\Delta\phi_{bulk}$, and a constant describing the conductance of the bulk solution, κ_D, by

$$\Delta\phi_{bulk} = '' - '' \frac{J_{charge}}{\kappa_D\cdot c_{bulk}}. \quad (25)$$

we set up an overall salt balance over the bulk solution in the cell, which is operated in batch mode, given by

$$2\cdot V_{bulk}\cdot\frac{\partial c_{bulk}}{\partial t} = -A_e\sum_{e=an,ca} J_{ions,e} \quad (26)$$

where V_{bulk} is the volume of the bulk solution and where e runs over the anode, *an*, and cathode, *ca*. To complete the description of the CDI cell we consider that

$$c_{mA} = c_{bulk}. \quad (27)$$

Equations (13)–(27) are the basis of the dynamic theory of salt adsorption in CDI. For MCDI, we include membranes and consider non-ideal permselectivity (i.e., besides counterions, co-ions can also go through the membranes). Therefore, the flux of ions through the membrane is calculated using the Nernst–Planck equation. We assume that:

- at each position in the membrane, the electroneutrality condition holds, $c_{mem,cation} - c_{mem,anion} + \omega X = 0$, where ωX is the membrane fixed charge defined per unit aqueous phase [37,38];
- the concentration profile and potential profile across the membrane are linear, which is highly correct for \omega X very large;
- the cat- and anion have equal diffusion coefficients;
- the transport of ions through the membranes can be described in steady state condition.

These assumptions lead to an expression for J_{ions} given by [39].

$$J_{ions} = -\kappa_{mem}\cdot(\Delta c_{T,mem} - \omega X\cdot\Delta\phi_{mem}) \quad (28)$$

where κ_{mem} is the membrane transport rate constant, which is directly linked to the membrane porosity and thickness, and to the mobility of ions within membrane pores. The term $\Delta c_{T,mem}$ is the difference between the total ion concentration in the membrane at the membrane-macropore interface, $c_{T,mem-elec}$, and in the membrane at the membrane-bulk solution interface, $c_{T,mem-bulk}$, and $\Delta\phi_{mem}$ is the difference in potential between the aforementioned interfaces.

The concentration at each membrane interface (membrane/bulk, $mem-bulk$, and membrane/electrode, $mem-elec$), $c_{T,mem}$, is given by [38].

$$c_{T,mem-bulk} = \sqrt{X^2 + (2\cdot c_{bulk})^2}$$
$$c_{T,mem-elec} = \sqrt{X^2 + (2\cdot c_{mA})^2}. \quad (29)$$

The potential drop over the membrane, $\Delta\phi_{mem}$, is related to ionic current density and average membrane concentration, $c_{T,mem}$, by

$$J_{charge} = -\kappa_{mem}\cdot c_{T,mem}\cdot\Delta\phi_{mem}. \quad (30)$$

The ionic current density, J_{charge}, is invariant across membranes and bulk solution. Therefore, the value of J_{charge} in Eqs. (24), (25) and (30) is the same.

At the $mem-bulk$ and $mem-elec$ interfaces, we consider Donnan equilibrium [40]. The Donnan potential, $\Delta\phi_D$, at these interfaces is given by

$$\Delta\phi_{D,mem-bulk} = \operatorname{asinh}\left(\frac{\omega X}{2\cdot c_{bulk}}\right)$$
$$\Delta\phi_{D,mem-elec} = \operatorname{asinh}\left(\frac{\omega X}{2\cdot c_{mA}}\right). \quad (31)$$

Finally, the cell voltage is calculated according to

$$\frac{V_{cell}}{V_T} = (\Delta\phi_{EDL} + \Delta\phi_{mem} + \Delta\phi_{D,mem-bulk} - \Delta\phi_{D,mem-elec})_{an} - (\Delta\phi_{EDL} + \Delta\phi_{mem} + \Delta\phi_{D,mem-bulk} - \Delta\phi_{D,mem-elec})_{ca} + \Delta\phi_{bulk}. \quad (32)$$

3. Experimental

3.1. Preparation of wire electrodes

All experiments in this study were performed using wire-shaped electrodes. Graphite rods (Poco EDM-3, diameter ~ 3.0 mm, Saturn Industries, Inc., USA) were used as an inner support and current collector. These graphite rods were coated with a porous carbon layer using a carbon slurry. A polymeric binder, polyvinylidene fluoride (PVDF) (Kynar HSV 900, Arkema Inc., Philadelphia, PA), was dissolved in a solvent: either acetone or N-methyl-2-pyrrolidone (NMP). For the preparation of electrodes using acetone("A-electrodes") PVDF was dissolved in boiling acetone (56 °C) in a weight ratio PVDF: acetone of 1: 45 and stirred for 1 h. Thereafter, activated carbon (YP50-F, Kuraray Chemical, Japan) and carbon black (Vulcan XC72R, Cabot Corp., Boston, MA) were added to the solution in a weight ratio activated carbon: carbon black:PVDF of 85:5:10. The resulting slurry was stirred for an additional hour at 50 °C. Graphite rods were repeatedly dipped into the slurry until a carbon layer with a thickness of ~370 μm and a length of 12 cm was obtained. The coated electrodes were dried at 100 °C overnight. For the preparation of electrodes using NMP ("NMP-electrodes"), we followed the procedure described in Ref. [26].

3.2. Preparation of wire electrodes coated with ion-exchange membranes

Commercially available Fumion® ionomer (FumaTech GmbH, Germany) was used in this study; FKS for cation exchange membranes (CEM), and FAS for anion exchange membranes (AEM). Membranes were coated onto the A-electrodes by dipping the electrodes into the solution with ionomer. Three layers of ionomer were coated on the electrode. Each layer was dried before coating a new one. The thickness of the resulting membranes was ~100 μm. The membrane-coated electrodes were dried in a tubular oven with a temperature ramp from 60 °C to 120 °C for 3 h. Before use, the electrodes were soaked in a 20 mM NaCl solution for at least 24 h.

3.3. CDI and MCDI experiments

The CDI and MCDI experiments were conducted in a batch-wise operated wire-CDI cell. The cell consisted of three pairs of electrodes separated by a piece of non-electrically conductive material (1.5 mm thick) located at the top and bottom of the electrodes, Fig. 1a, to avoid electrical connection between anodes and cathodes. In CDI and MCDI experiments, aqueous solutions of NaCl with an initial concentration of 20 mM were continuously stirred and purged with nitrogen. The cell voltage was controlled and the current was measured using a potentiostat (Iviumstat, Ivium Technologies, the Netherlands). The conductivity of the solution was also monitored and its value recalculated according to a calibration curve to obtain salt concentration. To perform the experiments we followed three procedures that are described below.

3.3.1. Method i

To calculate salt adsorption, charge, and charge efficiency as a function of charging voltage, desalination experiments were conducted with alternating adsorption and desorption steps in the same container, while we continuously monitor the conductivity of the solution. During the adsorption step, we applied different charging voltages, V_{ch}, of 0.6, 0.8, 1.0 and 1.2 V, for 35 min. This time was long enough to assure that equilibrium was reached. During the desorption step, we short-circuited the electrodes for regeneration i.e., we applied a discharging voltage of 0 V for 35 min. For each charging voltage, we conducted four consecutive adsorption and desorption cycles, and we determined salt adsorption, charge, and charge efficiency of the last cycle. These equilibrium experiments were conducted with A- and NMP-electrodes. Results are presented in Fig. 2a–c.

3.3.2. Method ii

To evaluate salt adsorption, charge, and charge efficiency in a more realistic setting, with actual desalination, experiments were conducted in two different containers, one container for adsorption, and another container for desorption. At the beginning of each experiment, the volume and salt concentration of the two solutions were the same. For adsorption, a charging voltage of 1.2 V was applied for 35 min. For desorption, the electrodes were moved from the adsorption to the desorption container and short-circuited for 35 min. Each experiment consisted of four consecutive desalination cycles. In these experiments, at the end of each adsorption or desorption step, the electrodes are moved to the other container and the conductivity is measured. Results are presented in Fig. 2d–f and 3.

3.3.3. Method iii

To evaluate dynamic salt adsorption and charge, desalination cycles were conducted with consecutive adsorption and desorption steps in the same container, as in method i. We applied a charging voltage of 1.2 V for 1.1 h, and thereafter we short-circuited the electrodes for 1.1 h. The experiments were conducted with A-electrodes with and without coated membranes. Results are presented in Fig. 4.

4. Results and discussion

In the first part of this Section, we present results of equilibrium CDI experiments, conducted with A- and NMP-electrodes, as a function of charging voltage (method i), and results of experiments conducted during real desalination (method ii). We compare results of experiments with the amph-D model. In the second part, we show the dynamic evolution of salt adsorption and charge in (M) CDI, and compare the experimental data with our dynamic theory.

4.1. Performance A- and NMP-electrodes

Equilibrium experiments were conducted using A- and NMP-electrodes (method i and ii). Fig. 2 compares the performance of both sets of electrodes in terms of salt adsorption, charge, and charge efficiency. Panels **a**, **b**, and **c** show an increase of these variables as a function of charging voltage. Panels **d**, **e**, and **f** show data obtained when consecutive desalination cycles are carried out.

Compared to NMP-electrodes, salt adsorption and charge efficiency of A-electrodes are considerably lower. We considered two explanations for this behavior: i) differences in pore size distribution and ii) presence of an additional chemical surface charge, σ_{chem}, in the micropores of the carbon material for the A-electrode. To test the first explanation, we conducted gas sorption analysis to measure porosity and surface area of the electrodes. Results show no evidence of a significant difference in the physical structure between the two sets of electrodes, Table S·I.1.

The second explanation considers modification of the chemical surface on carbon particles during the fabrication of the electrodes using acetone. Carbon-oxygen groups are the main surface groups present in activated carbon (AC) [41]. Functional groups such as carboxyl, lactone, and phenol impart the acidic behavior of AC [14,42]. We assume that electrode preparation with acetone increases the number of acidic groups in the carbon pores. To

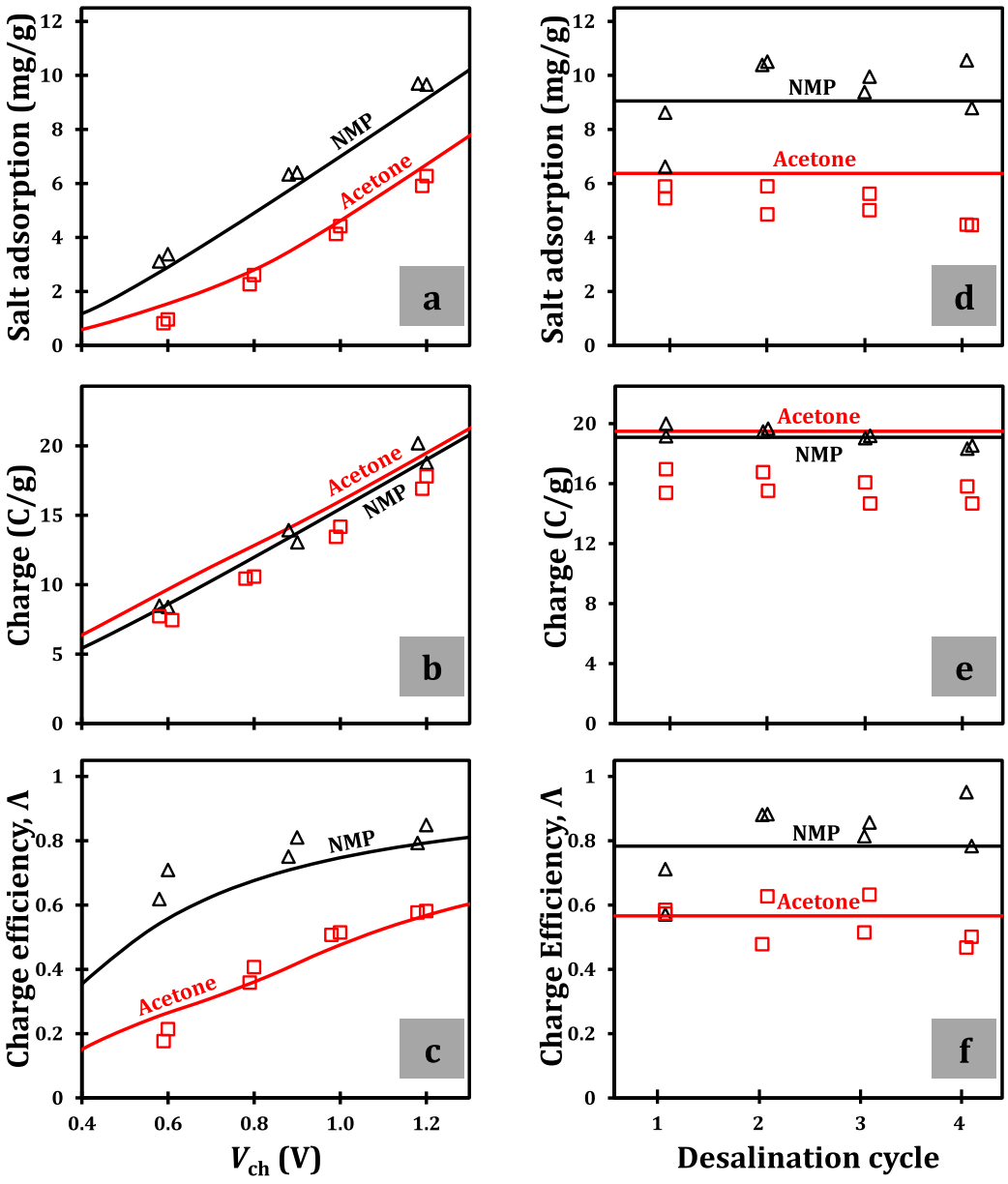

Fig. 2. Comparison of the amph-D theory (lines) with experimental data (symbols) for A- (squares) and NMP-electrodes (triangles); $c_{salt\ initial}$ = 20 mM. Equilibrium salt adsorption, charge, and charge efficiency as function of: a-c) charging voltage, V_{ch} (discharge 0 V, method i) and d-f) desalination cycle (method ii), see Section 3.3). Salt adsorption and charge are given per total mass of electrodes.

investigate this hypothesis, we measured the concentration of acidic groups in both sets of electrodes, NMP- and A-electrodes, following the procedure described in Ref. [17]. Results show, Figure S.I. 2, that the total concentration of acidic groups is about −0.43 M for A-electrodes and −0.18 M for NMP-electrodes. These results underline the possibility that acetone modifies the chemical surface of carbon electrodes by increasing the concentration of acidic surface groups. This increase may be responsible for the decrease in salt adsorption exhibited in experiments conducted with A-electrodes.

In our theory, we include the effect of chemical surface charge to predict salt adsorption and charge. For NMP-electrodes, we assumed that the density of acidic and basic surface charge groups is the same in value and opposite in sign. We used values for surface charge determined in Ref. [16], which is for the acidic region $\sigma_{chem,\ A} = -0.26$ M and for the basic region $\sigma_{chem,\ B} = +0.26$ M. For A-electrodes, we determined the chemical surface charge by adding to each region additional acidic groups with a concentration set to −0.35 M. The additional groups are assumed to be equally present in both A- and B-region in both anode and cathode. As shown in Fig. 2, the theory describes experimental data very closely for both types of electrodes, thus the amph-D model underpins that chemical surface charge has an impact on the performance of the electrodes [17].

Additional parameters required for the theory are micropore volume, υ_{mi}, which was measured using gas sorption and Stern layer capacitance , C_S, which was obtained from Ref. [25]. A list of all parameters is given in Tables 1 and 2.

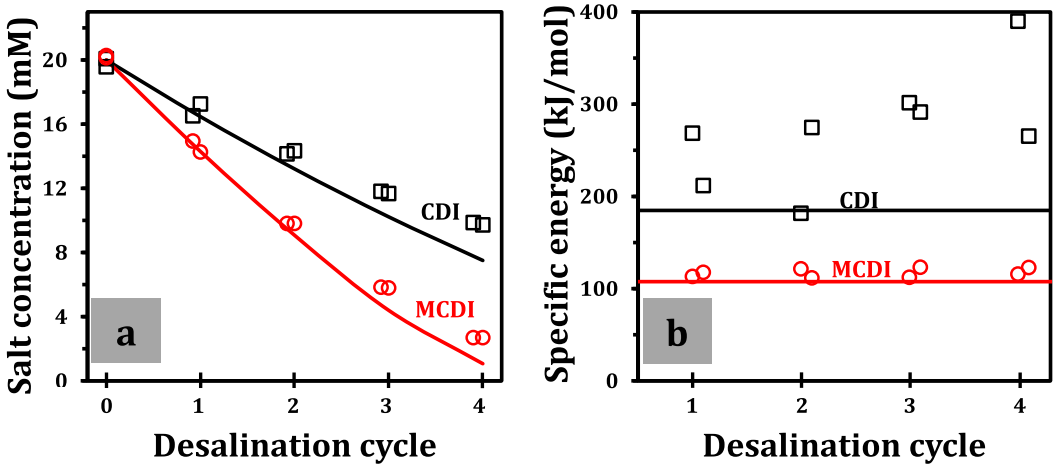

Fig. 3. a) Salt concentration in the bulk as function of the cycle number. Two sets of experiments (symbols) are compared with theory (lines), using Eqs. (1)–(12) for CDI and Eqs. (13)–(32) for MCDI. b) Specific energy, i.e., energy per salt removed. Data is reported for A-electrodes without ion-exchange membranes (CDI) and with membranes (MCDI).

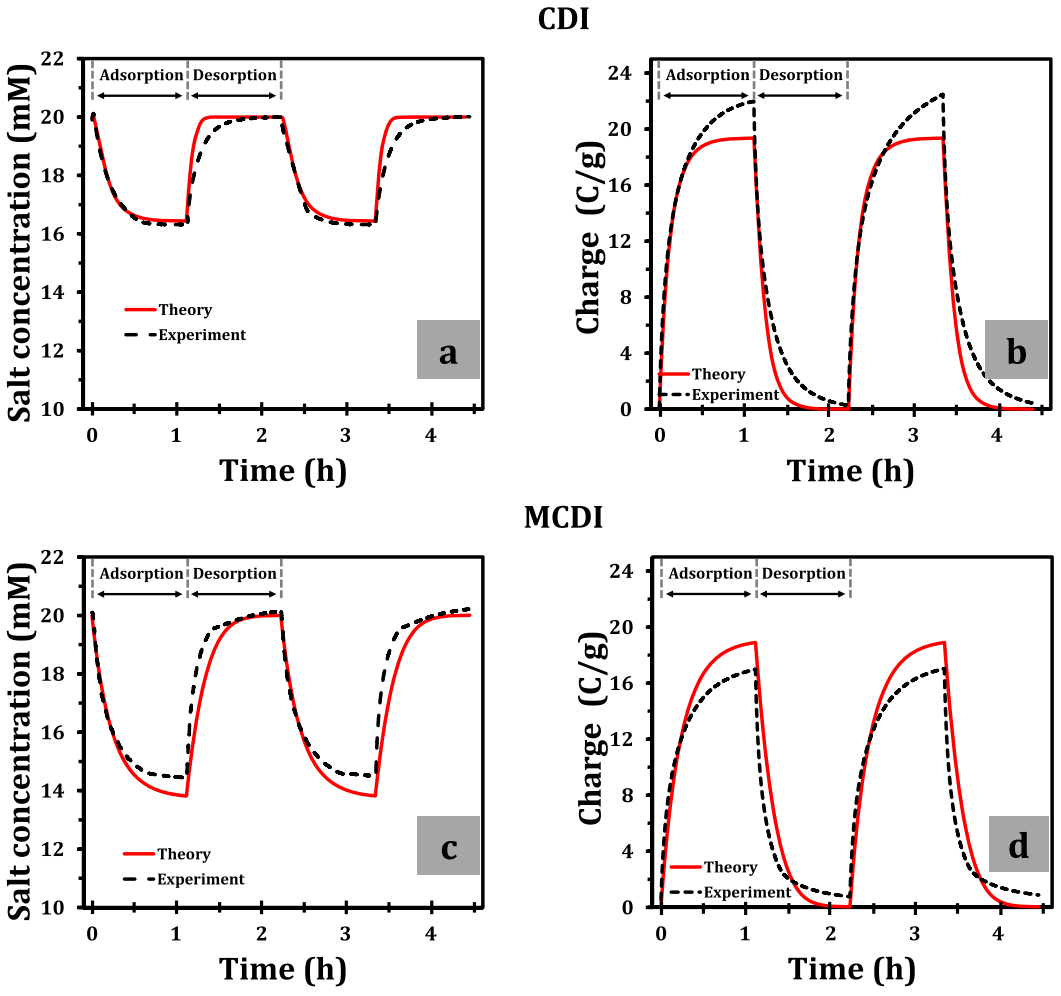

Fig. 4. Comparison of the dynamic theory with experimental data, all as a function of time. For CDI (A-electrodes without IEMs): a) salt concentration in the bulk, and b) charge per total mass of carbon. For MCDI, i.e., A-electrodes with ion-exchange membranes: c) salt concentration in the bulk, and d) charge per total mass of the carbon coating. From time 0 onwards, $V_{ch} = 1.2$ V is applied, which is reduced to zero for the desorption step.

Table 1
Parameters for A-electrodes.

Experimental			
λ_e	Thickness of porous carbon layer	1.83	mm
A_e	Area of electrode (cathode or anode)	6.90	cm^2
M_e	Total mass of porous carbon layer (anode and cathode)	1.27	g
ρ_{elec}	Electrode mass density	0.52	g/mL
V_{bulk}	Volume bulk solution	40	mL
amph-D theory			
$\sigma_{chem,A}$	Chemical surface charge - acidic region (−0.26–0.35)	−0.61	M
$\sigma_{chem,B}$	Chemical surface charge - basic region (+0.26–0.35)	−0.09	M
υ_{mi}	Micropore volume	0.49	mL/g
C_S	Stern capacitance	160	F/mL
Dynamic theory			
p_{mA}	Macroporosity	0.48	
p_{mi}	Microporosity	0.25	
ωX	Membrane charge density	(−)2.5	M
k	Kinetic rate constant for macropore-micropore transport	1	s^{-1}
κ_D	Fitting parameter for the conductance of the bulk solution	$2.7 \cdot 10^{-6}$	m/s
κ_{mem}	Membrane transport rate constant	$1.0 \cdot 10^{-8}$	m/s

4.2. Consecutive desalination cycles

Next, we show results of salt adsorption for CDI and MCDI experiments conducted with A-electrodes. These experiments were conducted by alternatingly transferring the electrodes from an adsorption to a desorption container, as described in Section 3.3 (method ii). Theory lines shown in Fig. 3a are based on equilibrium theory for CDI, and on dynamic theory for MCDI. The dynamic theory was adopted to include the non-ideal behavior of the IEMs. Fig. 3a shows the salt concentration in the container at the end of each adsorption step as a function of the number of desalination cycles. With IEMs, after 4 desalination cycles, we see a decrease in the initial salt concentration of about 87%, while for CDI the decrease was about 52%. Fig. 3b compares experimental data for energy consumption per mole of salt removed in CDI and MCDI. Energy consumption is calculated by integrating the current over time for the adsorption step and then multiplying by the charging voltage. As previously reported [27,43], IEMs do not only enhance the performance of the system by increasing the salt adsorption, but also decrease the energy required for the adsorption of ions. Our results show that MCDI requires, on average, 57% less energy to remove an ion than CDI. When we compare our data with data reported in Ref. [9] for CDI, we observe that the energy consumption in our system is higher. We attribute the increased energy consumption to the presence of additional acidic groups in the A-electrodes and to a higher resistance in bulk solution.

4.3. Dynamic salt adsorption

In this Section, we discuss experimental and theoretical results of dynamic ion adsorption in CDI and MCDI. For electrodes prepared with acetone, the theory includes parameters used in the amph-D model and additional parameters such as p_{mi}, p_{mA}, ωX, κ_D, κ_{mem}, and k. Porosities, p_{mi} and p_{mA}, are calculated as described in **S·I B**. The remaining parameters are treated as fitting parameters. When fitting κ_D and k using data from CDI experiments, we found that there is not a unique set of values that describe the experimental data, see Figure S·I 3a and S·I 3b. Consequently, we decided to set $k = 1\ s^{-1}$, which is in line with the approach taken in previous work [8,25] because when $k \geq 1\ s^{-1}$ there is no longer a rate limitation in the transport of ions from macro- to micropore; instead ion transport from macro- to micropore is at equilibrium.

With the value of k fixed, we then fitted κ_D. The values of ωX and κ_{mem} were fitted with MCDI experimental data. Both CDI and MCDI calculations include the additional surface charge that we assumed is present in A-electrodes.

Despite the fact that our theory describes CDI and MCDI data reasonably well, Fig. 4, it is unclear whether the ion transport from macro- to micropore is rate-limiting since more than one set of values for k and κ_D can closely describe our experimental data.

Although we did not include in our approach rate-limitation between macro- and micropores, this phenomenon may be important when we model ion adsorption in carbons with very small pores (sub-nm) [44], or thin electrodes with long macro- to micropore transport distances [1].

Table 2
Parameters for NMP-electrodes.

Experimental			
M_e	Total mass of porous carbon layer	0.90	g
ρ_{elec}	Electrode mass density	0.40	g/mL
V_{bulk}	Volume bulk solution	40	mL
amph-D theory [8]			
$\sigma_{chem,A}$	Chemical surface charge acid region	−0.26	M
$\sigma_{chem,B}$	Chemical surface charge base region	+0.26	M
υ_{mi}	Micropore volume	0.47	mL/g
C_S	Stern capacitance	160	F/mL

5. Conclusions

We extended dynamic theory for electrosorption of ions in porous carbon electrodes by including i) a chemical charge on the carbon surface to describe the electrical double layers and ii) a finite transport rate of ions from macro- to micropores. We used the theory to describe experimental data obtained in a CDI system. The CDI system has wire-shaped electrodes with and without coated ion-exchange membranes. As we showed, the extended theory closely describes fundamental aspects of desalination cycles: salt concentration and charge. Additionally, it also captures the influence of chemical surface groups on the performance of the electrode.

Regarding ion transport from macro- to micropores, it was not possible to verify the influence of this phenomenon on the dynamics of the electrosorption process. This is because numerically we found more than one set of values for the kinetic rate constant, k, and the conductance of the bulk solution, κ_D, that describe our experimental data to the same degree.

We also compared salt adsorption of electrodes fabricated using two solvents, namely acetone and N-methyl-2-pyrrolidone (NMP). Results show a lower salt adsorption for acetone-based electrodes

(A-electrodes). This difference is not explained by differences in pore size distribution or pore volumes. We suggest that the lower salt adsorption for A-electrodes is due to an increase in the density of acidic groups on the surface of the electrodes. Titration experiments indeed confirm that A-electrodes possess a higher concentration of acidic groups compared to NMP-electrodes.

Acknowledgments

This work was performed in the cooperation framework of Wetsus, European Centre of Excellence for Sustainable Water Technology (www.wetsus.nl). Wetsus is co-funded by the Dutch Ministry of Economic Affairs and Ministry of Infrastructure and Environment, the European Union Regional Development Fund, the Province of Fryslân, and the Northern Netherlands Provinces.

The authors like to thank the participants of the research theme Capacitive Deionization for fruitful discussions and financial support. The authors also like to thank F. Liu and M. Saakes for their advice in how to coat ion-exchange membranes on the carbon electrodes. T.M. Mubita acknowledges Wetsus Academy for financial support through a Scholarship Grant Award.

The research is supported by the Dutch Technology Foundation STW, which is part of The Netherlands Organisation for Scientific Research, and which is partly funded by the Ministry of Economic Affairs (VENI grant no 15071).

Appendix A. Supplementary data

Supplementary data related to this article can be found at https://doi.org/10.1016/j.electacta.2018.03.082.

References

[1] M.E. Suss, S. Porada, X. Sun, P.M. Biesheuvel, J. Yoon, V. Presser, Water desalination via capacitive deionization: what is it and what can we expect from it? Energy Environ. Sci. (2015) 2296–2319.
[2] O.N. Demirer, R.L. Clifton, C.A.R. Perez, R. Naylor, C. Hidrovo, Characterization of ion transport and -sorption in a carbon based porous electrode for desalination purposes, J. Fluids Eng (2013) 041201.
[3] C. Huyskens, J. Helsen, A.B. de Haan, Capacitive deionization for water treatment: screening of key performance parameters and comparison of performance for different ions, Desalination 328 (2013) 8–16.
[4] H. Li, Y. Gao, L. Pan, Y. Zhang, Y. Chen, Z. Sun, Electrosorptive desalination by carbon nanotubes and nanofibres electrodes and ion-exchange membranes, Water Res. (2008) 4923–4928.
[5] J.-H. Lee, W.-S. Bae, J.-H. Choi, Electrode reactions and adsorption/desorption performance related to the applied potential in a capacitive deionization process, Desalination (2010) 159–163.
[6] R.A. Rica, R. Ziano, D. Salerno, F. Mantegazza, D. Brogioli, Thermodynamic relation between voltage-concentration dependence and salt adsorption in electrochemical cells, Phys. Rev. Lett. 109 (2012), 156103.
[7] A.M. Johnson, J. Newman, Desalting by means of porous carbon electrodes, J. Electrochem. Soc. 118 (1971) 510–517.
[8] T. Kim, J.E. Dykstra, S. Porada, A. van der Wal, J. Yoon, P.M. Biesheuvel, Enhanced charge efficiency and reduced energy use in capacitive deionization by increasing the discharge voltage, J. Colloid Interf. Sci (2015) 317–326.
[9] R. Zhao, P.M. Biesheuvel, A. van der Wal, Energy consumption and constant current operation in membrane capacitive deionization, Energy Environ. Sci. 5 (2012) 9520–9527.
[10] H. Wang, L. Pilon, Accurate simulations of electric double layer capacitance of ultramicroelectrodes, J. Phys. Chem. C 115 (2011) 16711–16719.
[11] K.B. Oldham, A Gouy–Chapman–Stern model of the double layer at a (metal)/(ionic liquid) interface, J. Electroanal. Chem. 613 (2008) 131–138.
[12] R. Zhao, M. van Soestbergen, H.H.M. Rijnaarts, A. van der Wal, M.Z. Bazant, P.M. Biesheuvel, Time-dependent ion selectivity in capacitive charging of porous electrodes, J. Colloid Interface Sci. 384 (2012) 38–44.
[13] P.M. Biesheuvel, S. Porada, M. Levi, M.Z. Bazant, Attractive forces in microporous carbon electrodes for capacitive deionization, J. Solid State Electr (2014) 1365–1376.
[14] L. Wang, P.M. Biesheuvel, S. Lin, Reversible thermodynamic cycle analysis for capacitive deionization with modified Donnan model, J. Colloid Interface Sci. 512 (2018) 522–528.
[15] R.A. Rica, D. Brogioli, R. Ziano, D. Salerno, F. Mantegazza, Ions transport and adsorption mechanisms in porous electrodes during capacitive-mixing double layer expansion (CDLE), J. Phys. Chem. C 116 (2012) 16934–16938.
[16] P.M. Biesheuvel, Activated Carbon is an Electron-conducting Amphoteric Ion Adsorbent, 2015. Arxiv, 1509.06354.
[17] X. Gao, S. Porada, A. Omosebi, K.L. Liu, P.M. Biesheuvel, J. Landon, Complementary surface charge for enhanced capacitive deionization, Water Res. 92 (2016) 275–282.
[18] M. Müller, B. Kastening, The double layer of activated carbon electrodes. Part 1. The contribution of ions in the pores, J. Electroanal. Chem. 374 (1994) 149–158.
[19] S. Porada, M. Bryjak, A. van der Wal, P.M. Biesheuvel, Effect of electrode thickness variation on operation of capacitive deionization, Electrochim. Acta (2012) 148–156.
[20] X. Gao, A. Omosebi, J. Landon, K. Liu, Enhanced salt removal in an inverted capacitive deionization cell using amine modified microporous carbon cathodes, Environ. Sci. Technol. 49 (2015) 10920–10926.
[21] Y. Bouhadana, E. Avraham, M. Noked, M. Ben-Tzion, A. Soffer, D. Aurbach, Capacitive deionization of NaCl solutions at non-steady-state conditions: inversion functionality of the carbon electrodes, J. Phys. Chem. C 115 (2011) 16567–16573.
[22] A. Omosebi, X. Gao, J. Rentschler, J. Landon, K. Liu, Continuous operation of membrane capacitive deionization cells assembled with dissimilar potential of zero charge electrode pairs, J. Colloid Interface Sci. 446 (2015) 345–351.
[23] M. Mirzadeh, F. Gibou, T.M. Squires, Enhanced charging kinetics of porous electrodes: surface conduction as a short-circuit mechanism, Phys. Rev. Lett. (2014) 097701.
[24] M.E. Suss, P.M. Biesheuvel, T.F. Baumann, M. Stadermann, J.G. Santiago, In situ spatially and temporally resolved measurements of salt concentration between charging porous electrodes for desalination by capacitive deionization, Environ. Sci. Technol. 48 (2014) 2008–2015.
[25] J.E. Dykstra, R. Zhao, P.M. Biesheuvel, A. van der Wal, Resistance identification and rational process design in capacitive deionization, Water Res. 88 (2016) 358–370.
[26] S. Porada, B.B. Sales, H.V.M. Hamelers, P.M. Biesheuvel, Water desalination with wires, J. Phys. Chem. Lett. 3 (2012) 1613–1618.
[27] Y. Zhao, Y. Wang, R. Wang, Y. Wu, S. Xu, J. Wang, Performance comparison and energy consumption analysis of capacitive deionization and membrane capacitive deionization processes, Desalination 324 (2013) 127–133.
[28] ATSDR (Agency for Toxic Substances and Disease Registry), Toxicological Profile for Acetone, U.S. Department of Health and Human Services, Atlanta,GA, 1994.
[29] A. Jouyban, M.A.A. Fakhree, A. Shayanfar, Review of pharmaceutical applications of N-Methyl-2-Pyrrolidone, J. Pharm. Pharmaceut. Sci. 13 (2010) 524–535.
[30] P.M. Biesheuvel, H.V.M. Hamelers, M.E. Suss, Theory of water desalination by porous electrodes with immobile chemical charge, Colloids Interface Sci. Commun. 9 (2015) 1–5.
[31] H.P. Boehm, Some aspects of the surface chemistry of carbon blacks and other carbons, Carbon 32 (1994) 759–769.
[32] J.L. Figueiredo, M.F.R. Pererira, M.M.A. Freitas, J.J.M. Orfao, Modification of the surface chemistry of activated carbons, Carbon 37 (1999) 1379–1389.
[33] I. Cohen, E. Avraham, Y. Bouhadana, A. Soffer, D. Aurbach, Long term stability of capacitive de-ionization processes for water desalination: the challenge of positive electrodes corrosion, Electrochim. Acta 106 (2013) 91–100.
[34] M.V. Lopez-Ramon, F. Stoeckli, C. Moreno-Castilla, F. Carrasco-Marin, On the characterization of acidic and basic surface sites on carbons by various techniques, Carbon 37 (1999) 1215–1221.
[35] W. Tang, P. Kovalsky, D. He, T.D. Waite, Fluoride and nitrate removal from brackish groundwaters by batch-mode capacitive deionization, Water Res. 84 (2015) 342–349.
[36] E.J.F. Dickinson, R.G. Compton, Influence of the diffuse double layer on steady-state voltammetry, J. Electroanal. Chem. 661 (2011) 198–212.
[37] J.E. Dykstra, P.M. Biesheuvel, H. Bruning, A. Ter Heijne, Theory of ion transport with fast acid-base equilibrations in bioelectrochemical systems, Phys. Rev. E Stat. Nonlin. Soft Matter Phys. 90 (2014), 013302.
[38] A.H. Galama, J.W. Post, M.A. Cohen Stuart, P.M. Biesheuvel, Validity of the Boltzmann equation to describe Donnan equilibrium at the membrane–solution interface, J. Membr. Sci. 442 (2013) 131–139.
[39] R. Zhao, O. Satpradit, H.H.M. Rijnaarts, P.M. Biesheuvel, A. van der Wal, Optimization of salt adsorption rate in membrane capacitive deionization, Water Res. 47 (2013) 1941–1952.
[40] J.M. Paz-Garcia, J.E. Dykstra, P.M. Biesheuvel, H.V.M. Hamelers, Energy from CO2 using capacitive electrodes – a model for energy extraction cycles, J. Colloid Interface Sci. 442 (2015) 103–109.
[41] R.C. Bansal, M. Goyal, Activated Carbon Adsorption, CRC Press, 2005.
[42] Z. Chen, H. Zhang, C. Wu, Y. Wang, W. Li, A study of electrosorption selectivity of anions by activated carbon electrodes in capacitive deionization, Desalination 369 (2015) 46–50.
[43] H. Li, L. Zou, Ion-exchange membrane capacitive deionization: a new strategy for brackish water desalination, Desalination 275 (2011) 62–66.
[44] R.K. Kalluri, M.M. Biener, M.E. Suss, M.D. Merrill, M. Stadermann, J.G. Santiago, T.F. Baumann, J. Biener, A. Striolo, Unraveling the potential and pore-size dependent capacitance of slit-shaped graphitic carbon pores in aqueous electrolytes, Phys. Chem. Chem. Phys. 15 (2013) 2309.